

From Tides to Mixing Along the Hawaiian Ridge

Daniel L. Rudnick,^{1*} Timothy J. Boyd,² Russell E. Brainard,³
 Glenn S. Carter,⁴ Gary D. Egbert,² Michael C. Gregg,⁴
 Peter E. Holloway,⁵ Jody M. Klymak,² Eric Kunze,⁴ Craig M. Lee,⁴
 Murray D. Levine,² Douglas S. Luther,⁶ Joseph P. Martin,¹
 Mark A. Merrifield,⁶ James N. Moum,² Jonathan D. Nash,²
 Robert Pinkel,¹ Luc Rainville,¹ Thomas B. Sanford⁴

The cascade from tides to turbulence has been hypothesized to serve as a major energy pathway for ocean mixing. We investigated this cascade along the Hawaiian Ridge using observations and numerical models. A divergence of internal tidal energy flux observed at the ridge agrees with the predictions of internal tide models. Large internal tidal waves with peak-to-peak amplitudes of up to 300 meters occur on the ridge. Internal-wave energy is enhanced, and turbulent dissipation in the region near the ridge is 10 times larger than open-ocean values. Given these major elements in the tides-to-turbulence cascade, an energy budget approaches closure.

Turbulent mixing in the ocean interior has been observed to be too weak (1–3) to account for observed large-scale thermohaline structure (4–6). One hypothesis to account for this discrepancy posits that mixing is enhanced near rough topography. Elevated turbulence is found near seamounts (7, 8), ridges (9, 10), and passages (11). A likely source of energy for much of this mixing is the ocean tides. Recent inferences (12) from satellite altimeter data suggest that half of the 2 TW (1 TW = 10^{12} W) (13) required for ocean mixing can be derived from the tides. Mixing is envisioned as a cascade from surface tides, through internal tides and breaking internal waves, to turbulence.

Observing the tides-to-turbulence cascade in the ocean is a considerable challenge. Spatial scales range from megameters (the size of topographic features) down to centimeter scales, where molecular diffusion occurs. We approach this problem through an integrated program of modeling and observation focused on the Hawaiian Ridge. The Hawaii Ocean Mixing Experiment (HOME) includes observational components to survey the entire ridge, as well as to study far-field and

near-field regimes. The numerical modeling of surface and internal tides and the analysis of historical data complete the experimental approach. Here, we present key findings from a comprehensive survey of the ridge and from modeling of the internal tides.

The first element in the cascade is extraction of energy from the surface tide. The energy flux convergence of the surface tide is estimated from satellite altimetric measurements of surface height assimilated into a numerical tidal model (12, 14). The Hawaiian Ridge is one of the most prominent areas of deep-ocean surface tidal energy loss, at 20 ± 6 GW. A larger total energy loss is observed in some other deep-ocean regions, such as the Mid-Atlantic Ridge, but the en-

ergy loss per unit of volume is considerably higher over the Hawaiian Ridge, which occupies a much smaller volume of ocean.

A convergence of surface tidal energy flux implies a divergence of internal tides and/or locally dissipated energy. Here, the internal tidal energy flux is estimated from full-depth profiles of velocity, temperature, and salinity collected at 14 stations along the 3000-m isobath to the north and south of the ridge. Stations sampled regions spanning a broad range of internal-energy fluxes as predicted by numerical simulations of the interaction between the surface semidiurnal tide and topography along the Hawaiian Ridge (15). Large depth-integrated energy fluxes F_E in the semidiurnal band (16) are found at French Frigate Shoals (8 to 39 kW m⁻¹), Kauai Channel (5 to 21 kW m⁻¹), and south of Nihoa Island (5 to 16 kW m⁻¹) (Fig. 1). Weaker energy fluxes are found at Necker Island (1.5 to 2.8 kW m⁻¹) and north and southeast of Nihoa (1.3 to 4 kW m⁻¹). In comparison, an average flux along the Hawaiian Ridge of 2.8 kW m⁻¹ is predicted from a linear tidal scattering model (17). Observed energy fluxes at each station generally agree to within 50% or 1 kW m⁻¹, whichever is larger, with those deduced from numerical simulations (15). The few model-data disagreements that exist are the result of one or more of the following factors: (i) inadequately resolved small-scale topography in the numerical simulations, (ii) the use of only semidiurnal principal lunar (M_2) and solar (S_2) constituents in the model simulations, (iii) contamination by nontidal internal waves in the observations, or (iv) low-frequency temporal variations in the semidiurnal energy near the ridge (18).

If the energy fluxes were driven by the tides, one might expect a fortnightly modulation with the spring-neap tidal cycle. A station located southeast of French Frigate Shoals that was

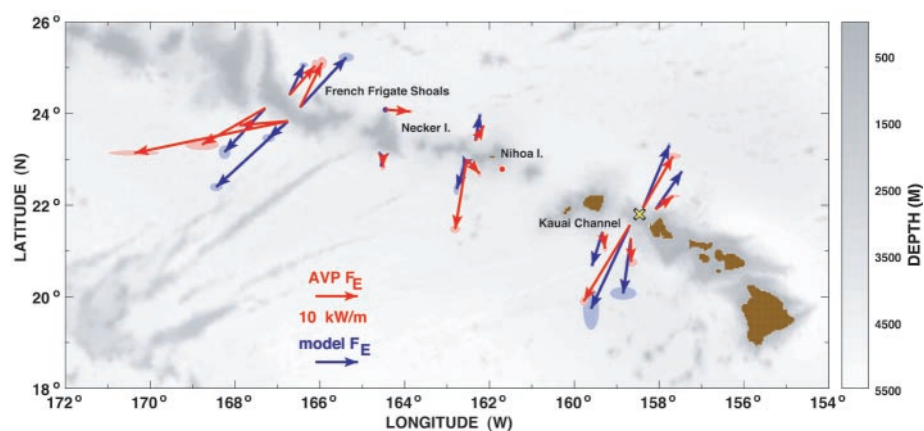


Fig. 1. Vertically integrated internal-wave energy fluxes from in situ profiles of velocity and density (red arrows), and from fortnightly semidiurnal tidal numerical simulations (blue arrows) in kilowatts per meter. Ellipses around the tips of the observational flux arrowheads denote jackknife standard errors calculated from the down profiles; ellipses around the numerical fluxes are the standard errors based on the closest model grid points and their four nearest neighbors. Fluxes range from 1.3 kW m⁻¹ southeast of Nihoa Island during neap to 39 kW m⁻¹ southeast of French Frigate Shoals during spring tide. The yellow cross marks the position of the mooring from which data are shown in Fig. 2.

¹ Scripps Institution of Oceanography, La Jolla, CA 92093-0213, USA. ² College of Oceanic and Atmospheric Sciences, Oregon State University, Corvallis, OR 97331, USA. ³ Honolulu Laboratory, Pacific Islands Fisheries Science Center, National Marine Fisheries Service (National Oceanic and Atmospheric Administration), 2570 Dole Street, Honolulu, HI 96822-2396, USA. ⁴ Applied Physics Laboratory, University of Washington, Seattle, WA 98105, USA. ⁵ School of Geography and Oceanography, University of New South Wales, Canberra ACT 2600, Australia. ⁶ Department of Oceanography, University of Hawaii, Honolulu, HI 96822, USA.

*To whom correspondence should be addressed. E-mail: drudnick@ucsd.edu

REPORTS

occupied twice shows such a modulation. Both occupations of this station confirm the large energy fluxes at this site. However, there is a marked difference in the flux direction between the observations and the model, and higher fluxes in the observations. Repeated measurements southwest of Nihoa Island also indicate larger fluxes at both spring and neap tides than the model predicts.

Internal waves are an intermediate step of the tides-to-turbulence cascade. Moored observations (19) on the ridge reveal internal waves with peak-to-peak amplitudes as large as 300 m at the semidiurnal period (Fig. 2). In addition, there are notable asymmetries in the semidiurnal oscillation, indicative of tidal harmonics and nonlinear dynamics. Variability extends up to frequencies of 1 cycle per hour. Spectral analysis indicates that amplitudes of these high-frequency waves are about a factor of 10 greater than open-ocean values (20, 21). Temporal and vertical structure in temperature contours suggests large vertical strain. At times, regions of very weak vertical temperature gradients are observed. In the active region extending 150 m above the bottom, temperature inversions with a vertical scale of 24 m or larger are present about 10% of the time.

Internal waves generated at the ridge propagate offshore to form a region of high internal-wave energy surrounding the ridge. Wide-ranging measurements of isopycnal displacement were obtained with SeaSoar, a towed vehicle that profiles over the upper 400 m. The total length of the SeaSoar tow exceeds 9000 km, allowing the calculation of internal-wave statistics in the upper 400 m as a function of position. The largest internal waves, during the spring tide, typically had peak-to-peak amplitudes of 60 m. Surveys of the Hawaiian Ridge in the Kauai Channel show large isopycnal displacements within about 100 km of the ridge (Fig. 3). This internal-wave energy is larger to the south. Isopycnal displacements are greatest about 50 to 100 km from the ridge crest, consistent with internal-tide propagation upward and southward from the southern edge of the ridge. The displacement maximum has variances at least a factor of 10 greater than open-ocean values, and they are most pronounced at depths below 200 m (22).

Whereas isopycnal displacements are dominated by large vertical-wavelength internal waves, it is through short vertical-wavelength shear that turbulence is generated. Shear was measured with a 50-kHz (12-m resolution) shipboard Doppler sonar. Shear shows the same asymmetry as does displacement, with larger variance to the south (Fig. 3). However, the largest shears, which are about four times as large as open-ocean values, are more tightly confined to the ridge. The across-ridge decay scale is shorter for shear than it is for displacement. This is

consistent with shear being dominated by short vertical wavelengths, which propagate more slowly and are dissipated locally.

The final stage of the energy cascade is the generation of small-scale turbulence. Turbulent energy dissipation rates ϵ were directly measured with a collection of profiling and towed instruments. These dissipation measurements were then averaged in across-ridge bins to define the structure of mixing at French Frigate Shoals (Fig. 4), a “hot spot” of especially strong dissipation along the Hawaiian Ridge. Diapycnal diffusivity is estimated from dissipation ϵ (23) as $K_p = 0.2 \epsilon N^{-2}$, where $N^2 = -g \rho_0^{-1} \partial\rho/\partial z$ is the square buoyancy frequency, ρ is potential density, and ρ_0 is a reference density.

Diffusivity at a depth of 500 m peaks at about $3 \times 10^{-4} \text{ m}^2 \text{ s}^{-1}$ over the ridge and then decays to background levels of $10^{-5} \text{ m}^2 \text{ s}^{-1}$ [typical of open-ocean diffusivity away from topography (7)] at a distance of 60 km from the shoals. The Hawaiian Ridge is thus a site of enhanced mixing, a conclusion supported by an analysis of historical data (24). Vertical profiles of dissipation are largest at the surface, have a minimum near 2000 m, and grow near the bottom. The resulting diffusivity shows a strong increase toward the bottom (Fig. 4), consistent with previous observations (9, 10), caused by increasing dissipation and decreasing buoyancy frequency. The turbulent diapycnal density flux $K_p \partial\rho/\partial z$ is directly proportional to ϵ , so turbu-

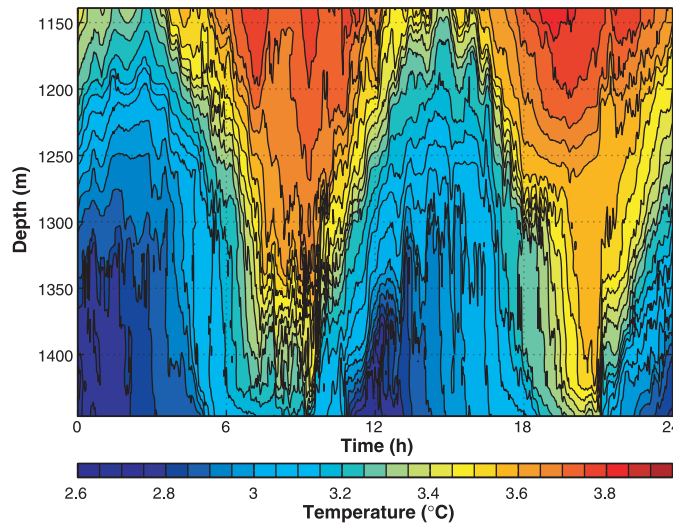


Fig. 2. Temperature as a function of depth and time, measured on a mooring on the flank of the ridge in water with a depth of 1453 m during spring tide. The position of the mooring is shown by the yellow cross in Fig. 1. At the semidiurnal period, the peak-to-peak displacements are 300 m.

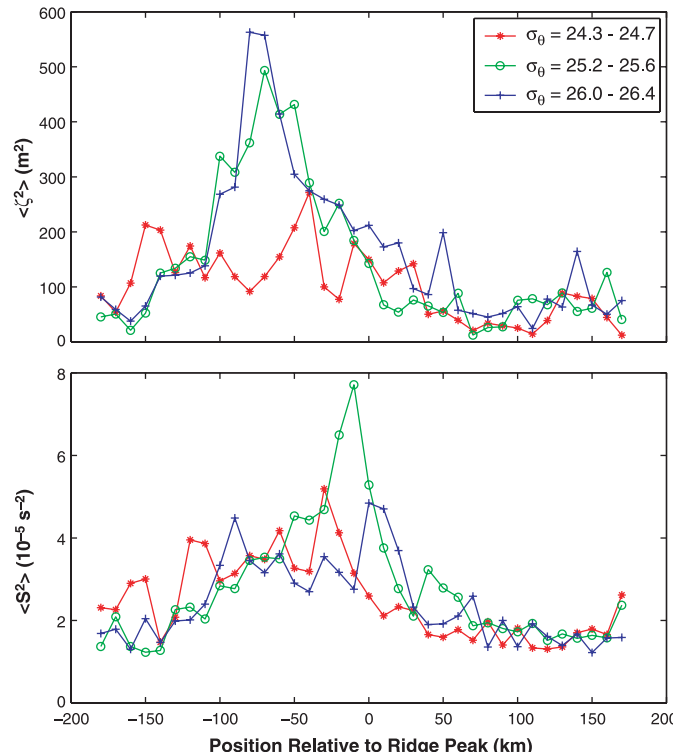


Fig. 3. Variances of isopycnal displacement (ζ) and shear (S) as functions of across-ridge distance (positive north) in the Kauai Channel. Individual averages, shown by the symbols, are obtained in bins of 10-km across-ridge distance. The three lines in each panel represent averages over the density (σ_θ) range indicated in the legend. The density ranges—24.3 to 24.7, 25.2 to 25.6, and 26.0 to 26.4 kg m^{-3} —have average depths of 110, 200, and 305 m, respectively. Regions of large displacement are located south of the ridge, and high shear is more tightly confined to the ridge.

lent density fluxes are largest near the surface.

The suite of observations and models allows an estimation of the terms in the tides-to-turbulence energy budget. There is a loss of 20 ± 6 GW from the M_2 surface tide along the length of the Hawaiian Ridge, as estimated from satellite altimetry assimilated into a tidal model (14). The 6-GW error in surface tidal loss is based on self-consistent errors in a Monte Carlo simulation (14). Encouraged by the comparison between the observed and modeled tidal internal-energy fluxes (Fig. 1), model results (25) are integrated to find an outgoing energy of 10 ± 5 GW (6 GW of which is associated with mode one, the vertical normal mode with one zero crossing in horizontal velocity) at the 4000-m isobath. The error estimate of 5 GW is based on the observed and modeled tidal internal-wave fluxes agreeing to within 50%.

Because 20 ± 6 GW are lost from the surface tide at the ridge and 10 ± 5 GW radiate away as internal tides to be dissipated elsewhere, the remainder is presumably dissipated locally. Calculation of the total local turbulent dissipation is challenging because dissipations are extremely variable and the sampling is sparse. An upper bound can be obtained by extrapolating measurements from French Frigate Shoals, where dissipations are strong, uniformly along the

ridge. Integrating the French Frigate Shoals dissipation across ridge and over depth, we obtain 4 kW m^{-1} . With a ridge length of 2500 km (26), an upper bound for local dissipation of 10 GW is implied. The local dissipation fortuitously makes up the balance between power supplied by the surface tide and that radiating away as internal tides, but it is an upper bound because most of the ridge is not as turbulent as French Frigate Shoals. Indeed, there are theoretical reasons to suspect that the bulk of the surface-tide loss will radiate away as internal waves with long vertical wavelengths (27), leaving only a small fraction to be lost locally to turbulence.

The HOME results have important implications for global ocean mixing. The 20 GW extracted from the surface tide at the Hawaiian Ridge is 1/50 of the global deep-water tidal loss of 1 TW, and thus tidal conversion at ridges is an important source of energy for mixing. A relevant question then is whether local mixing at isolated ridges is a major contributor to an average effective diffusivity of $10^{-4} \text{ m}^2 \text{ s}^{-1}$ implied by large-scale budgets (4–6). Because the average eddy diffusivity observed at the especially energetic French Frigate Shoals and other isolated rough topography (7–10) is at most about 2×10^{-4} to $3 \times 10^{-4} \text{ m}^2 \text{ s}^{-1}$, and the volume of the ocean occupied by rough topography cannot be more than 10%, the an-

swer seems to be no. We conclude that isolated ridges are important sinks for surface-tide energy and sites of elevated mixing, but cannot account for a global eddy diffusivity of $1 \times 10^{-4} \text{ m}^2 \text{ s}^{-1}$.

References and Notes

1. M. C. Gregg, *J. Geophys. Res.* **94**, 9686 (1989).
2. J. R. Ledwell, A. J. Watson, C. S. Law, *Nature* **364**, 701 (1993).
3. J. M. Toole, K. L. Polzin, R. W. Schmitt, *Science* **264**, 1120 (1994).
4. W. H. Munk, *Deep-Sea Res.* **13**, 707 (1966).
5. N. Hogg, P. Biscaye, W. Gardner, W. J. Schmitz, *J. Mar. Res.* **40**, 231 (1982).
6. D. Roemmich, S. Hautala, D. Rudnick, *J. Geophys. Res.* **101**, 14 (1996).
7. E. Kunze, J. M. Toole, *J. Phys. Oceanogr.* **27**, 2663 (1997).
8. R. G. Lueck, T. D. Mudge, *Science* **276**, 1831 (1997).
9. K. L. Polzin, J. M. Toole, J. R. Ledwell, R. W. Schmitt, *Science* **276**, 93 (1997).
10. J. N. Moum, D. R. Caldwell, J. D. Nash, G. D. Gundersen, *J. Phys. Oceanogr.* **32**, 2113 (2002).
11. K. L. Polzin, K. G. Speer, J. M. Toole, R. W. Schmitt, *Nature* **380**, 54 (1996).
12. G. D. Egbert, R. D. Ray, *Nature* **405**, 775 (2000).
13. W. Munk, C. Wunsch, *Deep-Sea Res.* **45**, 1977 (1998).
14. G. D. Egbert, R. D. Ray, *J. Geophys. Res.* **106**, 22 (2001).
15. M. A. Merrifield, P. E. Holloway, T. M. S. Johnston, *Geophys. Res. Lett.* **28**, 559 (2001).
16. At each station, 8 to 12 down and up profile pairs were collected over about 12 hours with the freefalling Absolute Velocity Profiler (AVP) (28). Semidiurnal signals were isolated from the background internal waves by fitting 12-hour period sinusoids to the profile time series at each depth. The fits were used to calculate the internal-wave energy flux $\langle v'p' \rangle$, where the internal perturbation velocity $v'(z)$ is relative to the time and depth means at each station, and the pressure anomaly $p'(z)$ is deduced from vertical displacements of isopycnals, assuming a hydrostatic balance (valid at tidal frequencies). The average $\langle \cdot \rangle$ is over wave phase (in this case, the 12-hour station occupation).
17. E. G. Morozov, *Deep-Sea Res.* **42**, 135 (1995).
18. G. T. Mitchum, S. M. Chiswell, *J. Geophys. Res.* **105**, 28 (2000).
19. T. Boyd, M. D. Levine, S. R. Gard, W. Waldorf, "Mooring observations from the Hawaiian Ridge, Nov. 2000–Jan. 2001," *Tech. Report No. Ref. 2002-1, Data report 185* (Oregon State University, Corvallis, OR, 2002).
20. W. Munk, in *Evolution of Physical Oceanography*, B. A. Warren, C. Wunsch, Eds. (MIT Press, Cambridge, MA, 1981), pp. 264–291.
21. M. C. Gregg, E. Kunze, *J. Geophys. Res.* **94**, 9686 (1991).
22. Tides were not resolved by the SeaSoar tows because individual across-ridge sections took about 1 day to complete. The displacement variances were calculated by averaging over many sections spanning a few weeks and may thus reflect time scales that are long as compared with the tide. However, rapid changes evident in consecutive across-ridge sections suggest that the variability is primarily of a frequency that is comparable to or higher than the semidiurnal tide.
23. T. R. Osborn, *J. Phys. Oceanogr.* **10**, 83 (1980).
24. T. D. Finnigan, D. S. Luther, R. Lukas, *J. Phys. Oceanogr.* **32**, 2988 (2002).
25. M. A. Merrifield, P. E. Holloway, *J. Geophys. Res.* **107**, 10.1029/2001JC000996 (2002).
26. Using 2500 km as the ridge length is consistent with the ridge extent where energy is lost from the surface tide (14) and where there is a divergence of internal-wave flux (25).
27. L. St. Laurent, C. Garrett, *J. Phys. Oceanogr.* **32**, 2882 (2002).
28. T. B. Sanford, R. G. Drever, J. H. Dunlap, *J. Atmos. Ocean. Technol.* **2**, 110 (1985).
29. HOME is funded by NSF.

17 April 2003; accepted 17 June 2003

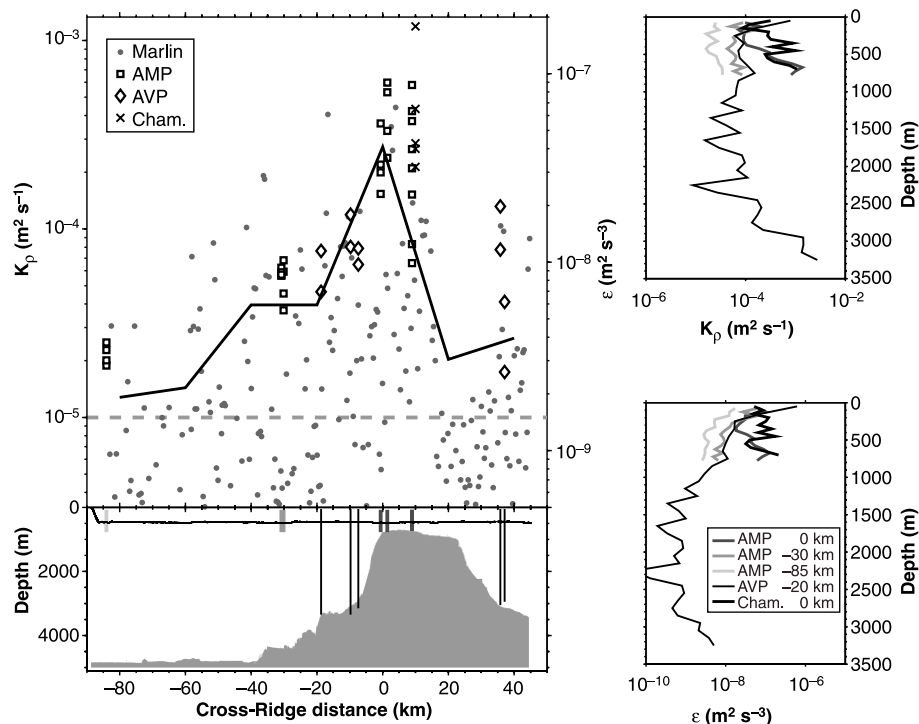


Fig. 4. Turbulent kinetic-energy dissipation rate ϵ and diapycnal diffusivity K_p , obtained across French Frigate Shoals over the depth range of 400 to 600 m (upper left panel; note the logarithmic axes). These measurements were made with four unique turbulence vehicles: AMP, AVP (28), and Chameleon are vertical profilers, and Marlin (8) is a towed vehicle. The solid line indicates the mean value of all of the data in 20-km lateral bins. The dashed line is the value of ϵ associated with the canonical abyssal diffusivity $K_p = 10^{-5} \text{ m}^2 \text{ s}^{-1}$ and square buoyancy frequency $N^2 = 3 \times 10^{-5} \text{ s}^{-2}$. Bottom depth and measurement locations (lower left panel) are shown as a function of cross-ridge distance. Vertical profiles of K_p and ϵ are shown in the upper and lower right panels, respectively.